ELSEVIER

Journal of Organometallic Chemistry 522 (1996) 249–257

Journal of Organometallic Chemistry

Reactivity of the cationic uranium amide compound $[U(\eta\text{-}C_8H_8)(NEt_2)(OC_4H_8)_2][BPh_4]$

Christophe Boisson [a], Jean Claude Berthet [a], Michel Ephritikhine [a,*], Monique Lance [b], Martine Nierlich [b]

[a] *Laboratoire de Chimie de l'Uranium, DSM, DRECAM, Service de Chimie Moléculaire, CNRS URA 331, CEA Saclay, 91191 Gif sur Yvette, France*

[b] *Laboratoire de Cristallographie, DSM, DRECAM, Service de Chimie Moléculaire, CNRS URA 331, CEA Saclay, 91191 Gif sur Yvette, France*

Received 9 January 1996

Abstract

The cationic uranium amide compound $[U(COT)(NEt_2)(THF)_2][BPh_4]$ **1** (COT = η-C_8H_8, THF = tetrahydrofuran) reacted with the nucleophiles MX ($LiCH(SiMe_3)_2$, $NaN(SiMe_3)_2$, KC_5H_5, KC_5Me_5, LiCl and KBH_4) to give the corresponding neutral addition complexes $[U(COT)(NEt_2)(X)]$. Insertion of CO_2, CS_2 or MeCN into the U–N bond of **1** afforded respectively $[U(COT)(E_2CNEt_2)(THF)_2][BPh_4]$ (E = O or S) and $[U(COT)(NC\{Me\}\{NEt_2\})(THF)_2][BPh_4]$. Reactions of **1** with the proton acidic molecules NEt_3HCl, C_5H_6 and ^iPrEH (E = O or S) led to the formation of $[U(COT)(Cl)(THF)_3][BPh_4]$, $[U(COT)(C_5H_5)(THF)_2][BPh_4]$ and $[U(COT)(E^iPr)_2]$ respectively. The crystal structures of $[U(COT)(NEt_2)(THF)_3][BPh_4]$ and $[U(COT)(S_2CNEt_2)(THF)_2][BPh_4]$ have been determined.

Keywords: Uranium; Amide; Cyclooctatetraene; Cation

1. Introduction

Recently we reported the new and efficient synthesis of cationic uranium compounds by protonolysis of a $U\text{–}NR_2$ bond with the ammonium salt NEt_3HBPh_4 [1,2]. The cationic amide complexes obtained from $[(M)(NR_2)_n]$ precursors deserve special attention because such species, which are very rare and limited to $[(M)\text{–}NHR]^+$ derivatives [3], are expected to be quite reactive; for example, organozirconium cations with heteroatom ligands have been shown to possess a potential utility in stoichiometric and catalytic processes [4]. We first examined the reactivity of the monocyclooctatetraene compound $[U(COT)(NEt_2)(THF)_2][BPh_4]$ **1** (COT = η-C_8H_8, THF = tetrahydrofuran) and here we present some derivatives that have been obtained by nucleophilic addition, by insertion of unsaturated molecules into the metal–nitrogen bond and by substitution of the amido group with proton acidic substrates. We also describe the crystal structures of $[U(COT)(NEt_2)(THF)_3][BPh_4]$ and $[U(COT)(S_2CNEt_2)(THF)_2][BPh_4]$.

2. Results and discussion

2.1. Reactions of $[U(COT)(NEt_2)(THF)_2][BPh_4]$ 1

The reactions of complex **1**, which are summarized in Scheme 1, have been performed in THF, toluene or diethyl ether, generally at 20 °C, although **1** was poorly soluble in these solvents; in contrast to $[U(COT)(NEt_2)_2(THF)]$, **1** could be dissolved in dichloromethane without decomposition. In the presence of a nucleophile X^-, the cationic species $[U(COT)(NEt_2)(THF)_2]^+$ was transformed into the corresponding neutral addition product $[U(COT)(NEt_2)(X)(THF)_x]$. The synthesis of the mixed ring compounds $[U(COT)(C_5R_5)(NEt_2)]$ (R = H, **2** or Me, **3**) by treatment of **1** with KC_5R_5 has already been reported [2]. The chloro- and tetrahydroborato-amide complexes $[U(COT)(NEt_2)(X)(THF)_x]$ (X = Cl, **4** or BH_4, **5**), which were readily formed from **1**

* Corresponding author.

PII S0022-328X(96)06280-8

upon addition of LiCl or KBH_4, were stable in THF solution but could not be isolated in the solid form, being decomposed into $[U(COT)_2]$ and other unidentified species by desolvation. Complex **4** was previously obtained by treating $[U(COT)(NEt_2)_2(THF)]$ with NEt_3HCl [5]; the behaviour of **5** is in contrast to that of the alkoxide analogues $[U(COT)(OR)(BH_4)]$ (R = Et, ^iPr, ^tBu) which were quite stable in the solid state [6].

Orange microcrystals of $[U(COT)(NEt_2)(CH\{SiMe_3\}_2)]$ **6**, a new example of a monocyclooctatetraene uranium alkyl compound [7], were isolated in 58% yield from the reaction of **1** and $LiCH(SiMe_3)_2$, whereas the brown sticky powder of the mixed bis-amide complex $[U(COT)(NEt_2)(N\{SiMe_3\}_2)]$ **7** was obtained from **1** and $NaN(SiMe_3)_2$ (72% yield).

Insertion of unsaturated molecules into the $M-NR_2$ bond is a classical reaction of metal amide compounds [8]. The carbamate complex $[U(COT)(O_2CNEt_2)_2]$ was thus synthesized by reacting $[U(COT)(NEt_2)_2(THF)]$ with carbon dioxide [5]. Similar treatment of **1** with CO_2 or CS_2 afforded the cationic carbamate and dithiocarbamate derivatives $[U(COT)(O_2CNEt_2)(THF)_x][BPh_4]$ **8** and $[U(COT)(S_2CNEt_2)(THF)_2][BPh_4]$ **9**; the latter was isolated as ochre microcrystals in 88% yield. Complex **1** reacted in THF with MeCN, giving orange crystals of the cationic aminido compound $[U(COT)(NC\{Me\}\{NEt_2\})(THF)_2][BPh_4]$ **10** (81% yield); in the IR spectrum, no absorption corresponding to free or coordinated MeCN was observed in the 2000–2500 cm^{-1} region and the strong band at 1524 cm^{-1} was attributed to the CN stretching vibration [9]. In contrast, treatment of the neutral precursor of **1**, $[U(COT)(NEt_2)_2(THF)]$, with 1 equivalent of MeCN induced rapid precipitation of an insoluble and not yet characterized crystalline complex resulting from protonation of the NEt_2 ligand, as shown by concomitant liberation of free NEt_2H (1 equivalent by NMR). Acetonitrile can in fact react with metal amides as an unsaturated molecule, giving the insertion aminido product [9] or/and as a protic species, giving the cyanoalkyl derivative [10]. The above results suggested that **1** was not very sensitive to acids.

Treatment of $[M]-NR_2$ complexes with proton acidic substrates HA provides a straightforward route to [M]–A derivatives [8], while the novel reaction of uranium amides with NEt_3HBPh_4 is useful for the synthesis of cationic compounds such as **1** [1,2]. By the way, it was interesting to note that protonation of the bis-amide compound $[U(COT)(NEt_2)(N\{SiMe_3\}_2)]$ **7** led to the selective formation of the cation $[U(COT)(N\{SiMe_3\}_2)(THF)_x]^+$ with liberation of NEt_2H (NMR experiment); it is clear that the steric bulk and electron withdrawing character of the trimethylsilyl group disfavour the approach of NEt_3H^+ onto the $N(SiMe_3)_2$ ligand. The cation $[U(COT)(N\{SiMe_3\}_2)(THF)_x]^+$ could not be obtained directly from **1** which was inert towards $(Me_3Si)_2NH$ at 20 °C. Attempts to prepare the dication $[U(COT)(THF)_x]^{2+}$ by treatment of **1** with NEt_3HBPh_4 or NH_4BPh_4 were unsuccessful. In the presence of NEt_3HCl, **1** was almost quantitatively transformed into $[U(COT)(Cl)(THF)_3][BPh_4]$ **11**, isolated as a brown microcrystalline powder; this reaction certainly proceeded by the intermediacy of the chloro-amide $[U(COT)(NEt_2)(Cl)(THF)_x]$ **4** which was then protonated with NEt_3HBPh_4. Synthesis of the mixed-ring cationic complex $[U(COT)(C_5H_5)(THF)_2][BPh_4]$ **12** by treating **1**

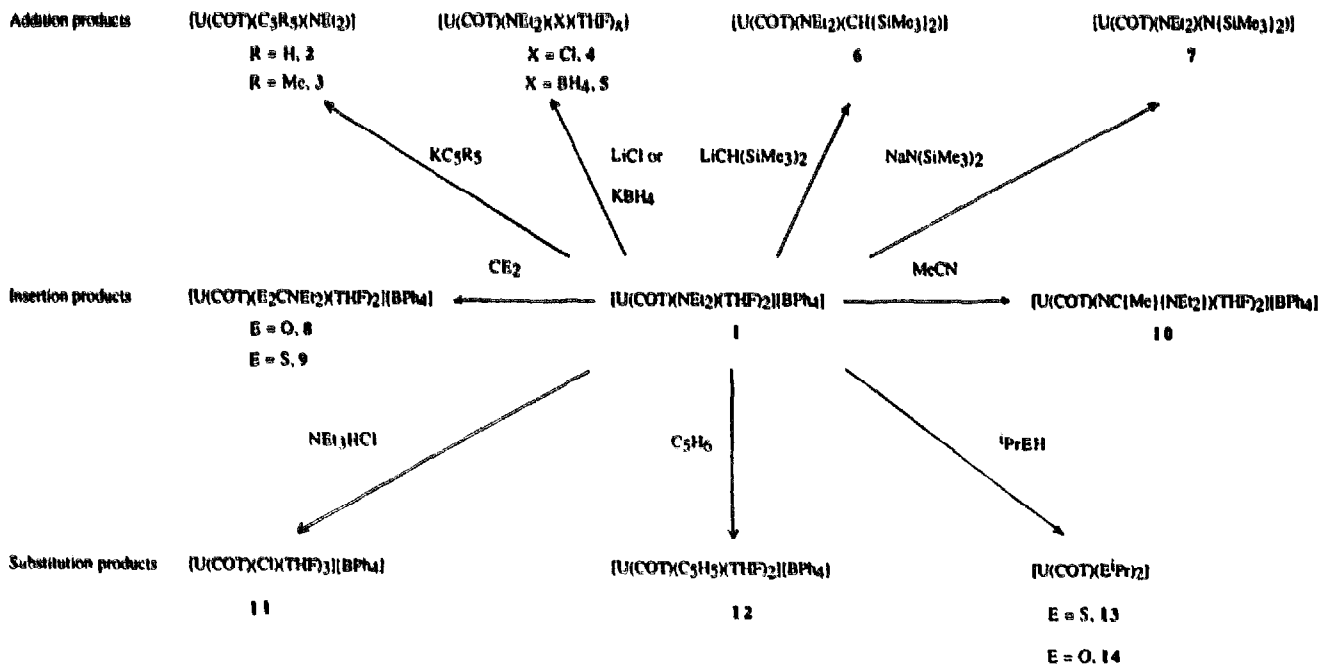

Scheme 1. Reactions of $[U(COT)(NEt_2)(THF)_2][BPh_4]$.

with cyclopentadiene has been previously reported [2]. This reaction required 60 h to go to completion, whereas formation of $[U(COT)(C_5H_5)(NEt_2)]$ from $[U(COT)(NEt_2)_2(THF)]$ and C_5H_6 was achieved after only 24 h at 20 °C [5]. Complex **1** was inert towards the less acidic phenylacetylene (pK_{as} of C_5H_6 and PhC≡CH are ca. 15 and 18.5 respectively [11]), in contrast to $[U(COT)(NEt_2)_2(THF)]$ which was readily transformed into $[U(COT)(NEt_2)(C{\equiv}CPh)]$ (NMR experiment) [12]. As expected from the acidity scale, **1** immediately reacted with ^{i}PrSH (pK_a *ca* 12) and was converted into the neutral bisthiolate compound $[U(COT)(S^iPr)_2]$ **13** [13]. Similar treatment of **1** with isopropanol, which has the same acidity as phenylacetylene, rapidly afforded the cationic alkoxide species $[U(COT)(O^iPr)(THF)_x]^+$; this could be characterized only by its NMR spectrum as it further reacted with ^{i}PrOH in the presence of NEt_2H to give $[U(COT)(O^iPr)_2]$ **14** [6]; the latter was also readily synthesized by alcoholysis of $[U(COT)(NEt_2)_2(THF)]$ [5]. The distinct reactivity of **1** towards isopropanol and phenylacetylene can be accounted for by initial coordination of ^{i}PrOH to the cation of **1**, giving $[U(COT)(NEt_2)(^iPrOH)]^+$, followed by proton transfer and elimination of NEt_2H; the intermediate $[U(COT)(O^iPr)(THF)_x]^+$ would itself coordinate an alcohol molecule and $[U(COT)(O^iPr)(^iPrOH)]^+$ would be deprotonated into $[U(COT)(O^iPr)_2]$ **14** by NEt_2H. Similar effects of coordination on acidity have recently been evidenced in the acid–base reactions between the uranium tris-amide $[U(N\{SiMe_3\}_2)_3]$ and various amines [14].

2.2. Characterization of the compounds; crystal structures of $[U(COT)(NEt_2)(THF)_3][BPh_4]$ and $[U(COT)(S_2CNEt_2)(THF)_2][BPh_4]$

The new complexes **5**–**11** were characterized by their elemental analyses (except **5** and **8**) and their ^{1}H NMR spectra (Table 1). In all compounds, the COT signal appears in the high field region, around δ −30; the resonances of the NEt_2 groups directly bound to the metal centre are visible at low field, near δ +30 and +100 for the CH_3 and CH_2 protons respectively. In the spectrum of the alkyl complex **6**, the signal corresponding to the hydrogen on the α carbon was too broad to be located; this methine resonance was also not detected in the spectra of $[U(C_5Me_5)_2(CH\{SiMe_3\}_2)]$ [15] and $[U(CH\{SiMe_3\}_2)_3]$ [16]. The spectrum of **10** exhibits magnetically nonequivalent ethyl groups, indicating that rotation about the CN bond is slow on the NMR time scale; this restricted rotation can be attributed to multiple CN bonding in hybrid B.

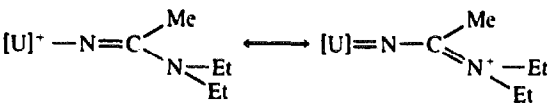

A B

Crystallization of **1** in THF afforded orange needles of $[U(COT)(NEt_2)(THF)_3][BPh_4]$ **15** which were transformed back into the orange powder of **1** when dried under vacuum. The crystals of **15** are composed of discrete cation–anion pairs. The BPh_4 anion displays

Table 1
^{1}H NMR spectra of compounds **5**–**11** [a]

Compound	Solvent	COT ligand [b]	Other ligands
$[U(COT)(NEt_2)(BH_4)(THF)_x]$ **5**	THF-d_8	−30.6	102.5 (4 H, CH_2); 35.7 (6 H, Me) −77.0 (4 H, $w_{1/2}$ ≈ 80 Hz, BH_4)
$[U(COT)(NEt_2)(CH\{SiMe_2\}_2)]$ **6**	benzene-d_6	−35.0	97.7 (4 H, $w_{1/2}$ ≈ 40 Hz, CH_2); 27.6 (6 H, Me) −24.38 (18 H, $SiMe_3$)
$[U(COT)(NEt_2)(N\{SiMe_3\}_2)]$ **7**	benzene-d_6	−34.3	84.3 (4 H, $w_{1/2}$ ≈ 40 Hz, CH_2); 27.78 (6 H, Me); −27.67 (18 H, $SiMe_3$)
$[U(COT)(O_2CNEt_2)(THF)_x][BPh_4]$ **8**	THF-d_8	−31.7	29.23 (4 H, CH_2); 15.45 (6 H, Me) 6.27 (20 H, Ph)
$[U(COT)(S_2CNEt_2)(THF)_2][BPh_4]$ **9**	THF-d_8	−34.0	11.44 (4 H, q, J = 7 Hz, CH_2); 4.76 (6 H, t, J = 7 Hz, Me) 6.35 (20 H, Ph)
$[U(COT)(NC(Me)(NEt_2)(THF)_2][BPh_4]$ **10**	pyridine-d_5	−28.3	61.3 (3 H, Me); 49.0 and 42.2 (2 H × 2, CH_2CH_3); 22.72 and 17.00 (3 H × 2, CH_2CH_3); 7.8 and 7.0 (20 H, Ph) 3.60 and 1.57 (8 H × 2, THF)
$[U(COT)(Cl)(THF)_2][BPh_4]$ **11**	pyridine-d_5	−33.0	6.7 (Ph and pyridine signals) 3.35 and 1.34 (12 H × 2, THF)

[a] At 30 °C, δ relative to TMS. When not specified, the signals are singlets with half-height widths between 10 and 30 Hz. [b] The signal integrates for 8 H.

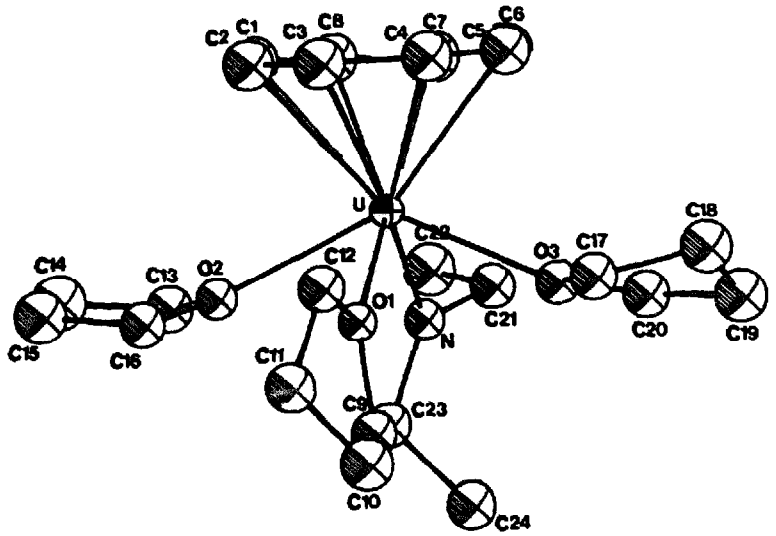

Fig. 1. ORTEP drawing of the cation $[U(COT)(NEt_2)THF)_3]^+$.

the expected geometry; an ORTEP [17] drawing of the cation is shown in Fig. 1 and selected bond distances and angles are listed in Table 2. The U–N bond distance, 2.18(2) Å, is similar to those determined in other cationic U(IV) amide compounds [1,2]. As usual in transition metal and uranium terminal amides, the nitrogen atom lies in the plane (within ±0.002 Å) defined by the metal and the two α carbons C(21) and C(23), whereas the U–N–C angles (120(1) and 125(1)°) and the C–N–C angle (115(1)°) deviate from the idealized value of 120° for a trigonal plane nitrogen atom.

The complex $[U(COT)(S_2CNEt_2)(THF)_2][BPh_4]$ **9** is the first uranium(IV) dithiocarbamate compound to have been crystallographically characterized; only the crystal structures of some anionic uranyl derivatives of formula $[UO_2(S_2CNR_2)_3]^-$ [18,19] have been reported. Here again, the structure consists of discrete cation–anion pairs; an ORTEP drawing of the cation is shown in Fig. 2 and selected bond distances and angles are listed in Table 2. The U–S bond distances (2.810(7) and 2.801(7) Å) compare favourably with the values of 2.80 and 2.87 Å determined in $[NMe_4][UO_2(S_2CNMe_2)_3]$ [18] or

Table 2
Selected bond distances (Å) and angles (deg) with estimated standard deviations for $[U(COT)(NEt_2)(THF)_2][BPh_4]$ and $[U(COT)(S_2CNEt_2)(THF)_2][BPh_4]$

$[U(COT)(NEt_2)(THF)_2][BPh_4]$					
U–N	2.18(2)	U–O(1)	2.48(1)	U–O(2)	2.53(1)
U–O(3)	2.56(1)	U–C(1)	2.72(2)	U–C(2)	2.72(2)
U–C(3)	2.78(2)	U–C(4)	2.75(2)	U–C(5)	2.73(2)
U–C(6)	2.67(2)	U–C(7)	2.67(2)	U–C(8)	2.67(2)
U–1 [a]	2.02(2)				
1–U–N	133.0(5)	1–U–O(1)	123.0(6)	1–U–O(2)	114.8(5)
1–U–O(3)	112.8(4)	N–U–O(1)	104.0(5)	N–U–O(2)	79.1(5)
N–U–O(3)	79.2(5)	O(1)–U–O(2)	72.8(4)	O(1)–U–O(3)	70.0(4)
O(2)–U–O(3)	130.3(4)				
$[U(COT)(S_2CNEt_2)(THF)_2][BPh_4]$					
U–S(1)	2.810(7)	U–S(2)	2.801(7)	U–O(1)	2.51(7)
U–O(2)	2.42(2)	U–C(1)	2.66(2)	U–C(2)	2.65(3)
U–C(3)	2.60(3)	U–C(4)	2.62(3)	U–C(5)	2.65(3)
U–C(6)	2.64(4)	U–C(7)	2.65(3)	U–C(8)	2.67(3)
U–1	1.93(3)	C(9)–S(1)	1.65(3)	C(9)–S(2)	1.68(3)
C(9)–N	1.46(3)				
1–U–O(1)	116.4(5)	1–U–O(2)	128.7(5)	1–U–S(1)	117.2(4)
1–U–S(2)	137.3(6)	S(1)–U–S(2)	63.4(2)	S(1)–U–O(1)	126.3(4)
S(1)–U–O(2)	77.0(4)	S(2)–U–O(1)	75.4(4)	S(2)–U–O(2)	93.8(5)
O(1)–U–O(2)	72.8(5)				

[a] 1 is the centroid of the COT ring.

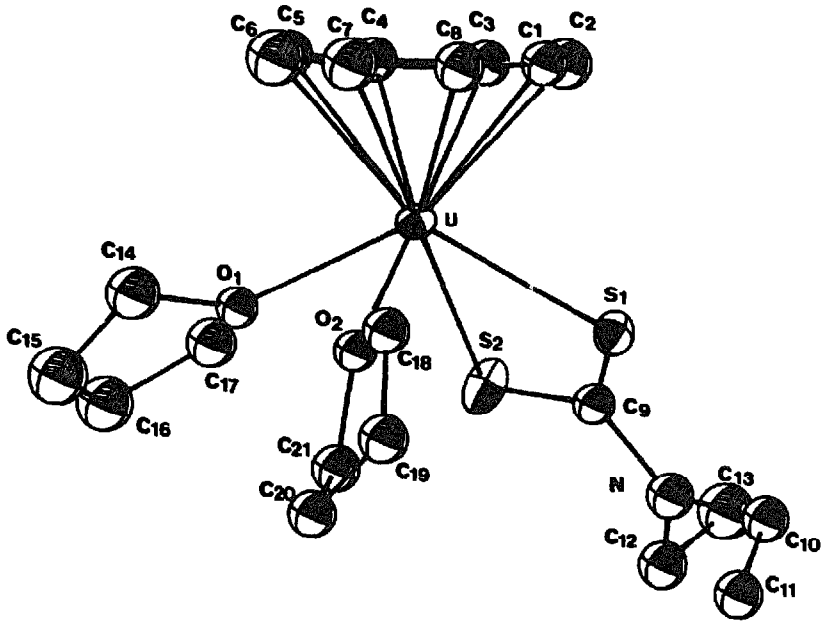

Fig. 2. ORTEP drawing of the cation $[U(COT)(S_2CNEt_2)(THF)_2]^+$.

$[Th(S_2CNEt_2)_4]$ [20]; the bite angle S(1)–U–S(2) is similarly equal to 63.4(2)°. As generally observed in the transition metal and f element dithiocarbamate compounds [21], the S(1), S(2), C(9), N, C(10) and C(12) atoms are coplanar (within ±0.03 Å); the U atom is 0.113(1) Å out of this plane. However, the C(9)–N distance of 1.46(3) Å and the C(9)–S distances of 1.68(3) and 1.65(3) Å appear respectively longer and shorter than the typical values of 1.35 and 1.75 Å. These distinct parameters suggest that hybrid C has a more important contribution to the true structure of **9**.

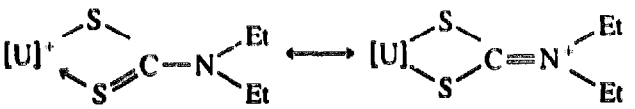

C D

In both compounds, the C_8H_8 rings are planar within ±0.03 Å and the uranium–carbon bond distances, which average 2.64(4) Å in **9** and 2.71(4) Å in **15** are within the range of U–C(COT) bond lengths which vary from 2.62 Å in $[U(COT)(S^iPr)_2]$ [13] and 2.70 Å in the U(III) compound $[U(COT)(C_5Me_5)(dmbipy)]$ (dmbipy = 4,4′-dimethyl-2,2′-bipyridine) [22]; the typical value of 2.68 Å is found in most of the cycloctatetraene U(IV) complexes [6,13,23] and also in the U(V) cation $[U(COT)(NEt_2)_2(THF)]^+$ [5]. These results confirm that these metal–ligand distances cannot be related to the formal oxidation state of the uranium centre [5].

3. Concluding remarks

The cationic uranium amide complex $[U(COT)(NEt_2)(THF)_2][BPh_4]$ **1** was interesting for the preparation of neutral derivatives of general formula $[U(COT)(NEt_2)(X)(THF)_x]$ which were obtained by nucleophilic addition of X^-. These syntheses further illustrate the practical use of cationic precursors in actinide chemistry, avoiding the problems with the tedious elimination of salts and formation of 'ate' complexes which are frequently encountered in the classical metathesis reaction of halide compounds with lithium or Grignard reagents [1,2]. The advantage of such cationic complexes is even more evident when the corresponding halide cannot be isolated, as in the case of $[U(COT)(NEt_2)(Cl)(THF)_x]$; in this context, it has also been reported that $[U(NEt_2)_3(Cl)]$ was not stable, being in equilibrium with $[U(NEt_2)_2(Cl)_2]$ and $[U(NEt_2)_4]$, in contrast to $[U(NEt_2)_3][BPh_4]$ which was a convenient starting material for a variety of derivatives [1,2]. Complex **1** was also useful to synthesize new cationic compounds by insertion of unsaturated molecules into the U–N bond; thus was obtained $[U(COT)(S_2CNEt_2)(THF)_2][BPh_4]$, the first dithiocarbamate compound of U(IV) to have been crystallographically characterized. Of special interest are the differences of reactivity between a cationic amide complex and its corresponding neutral precursor which would lead to selective synthesis of new derivatives. By comparison with $[U(COT)(NEt_2)_2(THF)]$, **1** was found to be less reactive towards cyclopentadiene or phenylacetylene, a fact that may be explained by the slower attack of the proton acidic molecule onto the positively charged species. However, rapid reaction occurred between **1** and isopropanol; in this case, possible coordination of the alcohol molecule onto the cation would decrease its pK_a and favour the cleavage of the U–N bond. Contrary to that observed with $[U(COT)(NEt_2)_2(THF)]$, acetonitrile did not proto-

nate the NEt_2 ligand of **1** but inserted into the U–N bond to give the aminido derivative $[U(COT)(NC(Me)(NEt_2))(THF)_2][BPh_4]$.

4. Experimental details

4.1. General methods

All preparations and reactions were carried out under argon (less than 5 ppm oxygen or water) using standard Schlenk-vessel and vacuum-line techniques or in a glove box. Solvents were thoroughly dried and deoxygenated by standard methods and distilled immediately before use. Deuterated solvents were dried over Na–K alloy.

Elemental analyses were performed by Analytische Laboratorien at Lindlar (Germany). The IR spectra were recorded in KBr plates on a Perkin–Elmer 1725X spectrometer. The ^1H NMR spectra were recorded on a Bruker WP 60 (FT) instrument and were referenced internally using the residual protio solvent resonances relative to tetramethylsilane (δ 0); the spectra are described in Table 1.

The commercial reagents were dried by standard methods before use. NEt_3HBPh_4 was prepared in water by mixing $NaBPh_4$ and NEt_3HCl; the white powder which precipitated was filtered off, washed successively with hot water and diethyl ether and dried under vacuum. $LiCH(SiMe_3)_2$ [24], $NaN(SiMe_3)_2$ [25] and the uranium complex **1** [2] were synthesized by published methods.

4.2. Reactions of 1 with LiCl and KBH_4

(a) An NMR tube was charged with **1** (9.7 mg, 0.011 mmol) and LiCl (0.5 mg, 0.011 mmol) in THF-d_8 (0.35 ml). After 15 min at 20 °C, the spectrum of the red solution showed the quantitative formation of **4**.

(b) An NMR tube was charged with **1** (8.0 mg, 0.009 mmol) and KBH_4 (0.5 mg, 0.009 mmol) in THF-d_8 (0.35 ml). After 15 min at 20 °C, the spectrum of the red solution showed that **1** was almost quantitatively transformed into **5**.

Complexes **4** and **5** were stable in solution but evaporation of the solvent led to their decomposition into $[U(COT)_2]$ and unidentified compounds.

4.3. Synthesis of $[U(COT)(NEt_2)(CH(SiMe_3)_2)]$ 6

A 50 ml round-bottomed flask was charged with **1** (339 mg, 0.38 mmol) and $LiCH(SiMe_3)_2$ (57 mg, 0.34 mmol) and diethyl ether (20 ml) was condensed into it under vacuum at −78 °C. The temperature was slowly raised to 20 °C, the mixture was stirred for 2 h and the orange solution was filtered and evaporated to dryness. The residue was extracted in diethyl ether (3 × 10 ml), the solvent evaporated off and the product extracted in diethyl ether (25 ml). After evaporation and drying under vacuum, **6** was isolated as orange needles (115 mg, 58%). Anal. Found: C, 39.94; H, 6.44; N, 2.32. $C_{19}H_{37}NSi_2U$. Calc.: C, 39.78; H, 6.50; N, 2.44%.

4.4. Synthesis of $[U(COT)(NEt_2)(N(SiMe_3)_2)]$ 7

A 50 ml round-bottomed flask was charged with **1** (300 mg, 0.34 mmol) and $NaN(SiMe_3)_2$ (62.7 mg, 0.34 mmol) and toluene (20 ml) was condensed into it under vacuum at −78 °C. The mixture was heated at 45 °C for 30 min and the red solution turned yellow. After 2 h at 20 °C, the solvent was evaporated off; the residue was dried under vacuum and then extracted in a mixture of pentane (20 ml) and toluene (15 ml). A brown pasty powder of **7** was obtained after evaporation to dryness (142 mg, 72%). Anal. Found: C, 37.46; H, 6.20; N, 4.73. $C_{18}H_{36}N_2Si_2U$. Calc.: C, 37.62; H, 6.31; N, 4.87%.

4.5. Reaction of 1 with CO_2

An NMR tube was charged with **1** (11 mg, 0.012 mmol) in THF-d_8 (0.35 ml) and was then adapted to the vacuum line, cooled at −78 °C, degassed and exposed to 1 atm of CO_2. After 1 h at 20 °C, the spectrum of the orange solution showed that **1** was totally transformed into $[U(COT)(O_2CNEt_2)(THF)_x][BPh_4]$ **8**.

4.6. Synthesis of $[U(COT)(S_2CNEt_2)(THF)_2][BPh_4]$ 9

A 50 ml round-bottomed flask was charged with **1** (250 mg, 0.28 mmol) in THF (20 ml) and CS_2 (65 μl, 1.04 mmol) was introduced via a microsyringe. The mixture was stirred for 3.5 h at 20 °C, giving a clear orange solution. Addition of diethyl ether (30 ml) caused precipitation of an ochre powder of **9** which was filtered off and dried under vacuum (239 mg, 88%). IR: 1514 (ν(CN)), 1357, 1240 and 991 cm^{-1}. Anal. Found: C, 56.53; H, 5.58; N, 1.40. $C_{45}H_{54}BNO_2S_2U$. Calc.: C, 56.66; H, 5.70; N, 1.47%.

4.7. Synthesis of $[U(COT)(NC(Me)(NEt_2))(THF)_2][BPh_4]$ 10

A 50 ml round-bottomed flask was charged with **1** (235 mg, 0.27 mmol) in THF (20 ml) and MeCN (24 μl, 0.46 mmol) was introduced via a microsyringe. The mixture was stirred at 85 °C for 10 h. The orange solution was filtered and the orange powder of **10** precipitated upon addition of pentane (20 ml); the product was filtered off and dried under vacuum (200 mg, 81%). IR: 1524 cm^{-1} (ν(CN)). Anal. Found: C, 59.85;

H, 6.11; N, 3.14. $C_{46}H_{57}BN_2O_2U$. Calc.: C, 60.13; H, 6.25; N, 3.05%.

4.8. Reaction of 7 with NEt_3HBPh_4

An NMR tube was charged with **7** (10.0 mg, 0.017 mmol) and NEt_3HBPh_4 (7.3 mg, 0.017 mmol) in THF-d_8 (0.35 ml). After 10 min at 20 °C, the spectrum of the red solution showed the signals of free NEt_2H (1 equivalent) and the resonances attributed to the cation $[U(COT)(N\{SiMe_3\}_2)(THF)_x]^+$. δ 6.0 (20 H, Ph), 2.05 (18 H, $SiMe_3$) and −32.64 (8 H, COT).

4.9. Synthesis of $[U(COT)(Cl)(THF)_3][BPh_4]$ 11

A 50 ml round-bottomed flask was charged with **1** (266 mg, 0.30 mmol) and NEt_3HCl (39 mg, 0.28 mmol) and THF (20 ml) was condensed into it under vacuum at −78 °C. The flask was immersed in an ultrasound bath (60 W, 40 kHz) for 3 min at 40 °C; after this period the mixture was magnetically stirred for 30 min at 20 °C. The red solution was filtered and its volume was reduced to 10 ml; addition of a 1:1 mixture of THF–diethyl ether (20 ml) caused the precipitation of a brown powder of **11**, which was filtered off, washed with diethyl ether and dried under vacuum (249 mg, 96%). Anal. Found: C, 57.49; H, 5.54; N, 4.10. $C_{44}H_{52}BClO_3U$. Calc.: C, 57.87; H, 5.74; N, 3.88%.

4.10. Reactions of 1 with ^{i}PrSH and ^{i}PrOH

(a) An NMR tube was charged with **1** (10 mg, 0.011 mmol) in THF-d_8 (0.35 ml) and ^{i}PrSH (2.0 μl, 0.022 mmol) was introduced via a microsyringe. After 10 min at 20 °C, the spectrum of the red solution showed that **1** was completely transformed into $[U(COT)(S^iPr)_2]$.

(b) An NMR tube was charged with **1** (13 mg, 0.015 mmol) in THF-d_8 (0.35 ml) and ^{i}PrOH (1.1 μl, 0.014 mmol) was introduced via a microsyringe. After 10 min at 20 °C, the spectrum of the red solution showed that **1** was partially transformed into a 35:65 mixture of $[U(COT)(O^iPr)_2]$ and $[U(COT)(O^iPr)(THF)_x][BPh_4]$; δ

Table 3
Crystallographic data and experimental details for $[U(COT)(NEt_2)(THF)_3][BPh_4]$ and $U(COT)(S_2CNEt_2)(THF)_2][BPh_4]$

	$[U(COT)(NEt_2)(THF)_3][BPh_4]$	$[U(COT)(S_2CNEt_2)(THF)_2][BPh_4]$
Crystal data		
Formula	$C_{48}H_{62}BNO_3U$	$C_{45}H_{54}BNO_2S_2U$
M	949.88	953.91
Crystal dimensions (mm)	0.45 × 0.35 × 0.15	0.50 × 0.40 × 0.25
Colour	red-orange	red
Crystal system	monoclinic	monoclinic
Space group	$P2_1/c$	$P2_1/n$
a (Å)	18.242(6)	8.847(2)
b (Å)	9.773(3)	21.840(1)
c (Å)	25.78(1)	22.013(5)
β (deg)	102.71(4)	90.43(2)
V (Å^3)	4483(4)	4253(2)
Z	4	4
d_{calc} (g cm^{-3})	1.407	1.489
μ(Mo Kα) (cm^{-1})	34.70	37.47
F(000)	1912	1920
Data collection		
Temperature (K)	294	294
θ limits (deg)	1, 20	1, 20
Scan type	$\omega, 2\theta$	$\omega, 2\theta$
Scan width	$0.8 + 0.35 \tan\theta$	$0.8 + 0.35 \tan\theta$
Range of abs. trans.	0.870, 0.999	0.893, 0.999
Range of h, k, l	0 to 17, 0 to 9, −24 to 24	0 to −8, 0 to 21, −21 to 21
Reflections collected		
Total	4879	4579
Unique	4180	3954
with $I > 3\sigma(I)$	2969	2008
Number of parameters	222	224
$R = \Sigma\|\|F_o\| - \|F_c\|\|/\Sigma\|F_o\|$	0.051	0.046
$Rw = [\Sigma w\|\|F_o\| - \|F_c\|\|^2/\Sigma w(\|F_o\|)^2]^{1/2}$	0.083	0.059
$w = 1/(\sigma F)^2 = 4F^2/[\sigma I^2 + (pF^2)^2]^{1/2}$	$w = 1$	$w = 1$
Max. residual electron density (e Å^{-3})	0.902	0.708

165.82 (1 H, CH), 61.89 (6 H, Me) and −31.19 (8 H, COT). After addition of a second equivalent of ^{i}PrOH, the spectrum showed that **1** was completely transformed into [U(COT)(O^{i}Pr)$_2$].

Table 4
Fractional atomic coordinates, thermal parameters and their estimated standard deviations for [U(COT)(NEt$_2$)(THF)$_3$][BPh$_4$]

	x	y	z	B_{eq}
U	0.16816(4)	0.22755(6)	0.32063(3)	2.52(1) [a]
O(1)	0.2750(6)	0.248(1)	0.3984(4)	3.2(3)
O(2)	0.2844(7)	0.145(1)	0.2916(5)	4.0(3)
O(3)	0.1492(7)	0.435(1)	0.3769(5)	3.8(3)
N	0.1856(8)	0.394(1)	0.2685(6)	3.5(3)
C(1)	0.130(1)	−0.017(2)	0.2721(9)	5.3(5)
C(2)	0.157(1)	−0.049(2)	0.3286(8)	5.2(5)
C(3)	0.139(1)	−0.003(2)	0.3761(9)	5.1(5)
C(4)	0.092(1)	0.093(2)	0.3859(8)	5.0(5)
C(5)	0.041(1)	0.185(2)	0.3579(8)	4.9(5)
C(6)	0.018(1)	0.218(2)	0.3055(9)	5.6(5)
C(7)	0.034(1)	0.178(2)	0.2570(9)	5.6(5)
C(8)	0.080(1)	0.082(2)	0.2439(9)	6.1(6)
C(9)	0.331(1)	0.361(2)	0.4037(8)	4.2(5)
C(10)	0.373(1)	0.342(3)	0.463(1)	6.7(6)
C(11)	0.373(1)	0.194(2)	0.4734(9)	5.4(5)
C(12)	0.293(1)	0.154(2)	0.4463(8)	4.3(5)
C(13)	0.289(1)	0.140(2)	0.2329(9)	5.4(5)
C(14)	0.340(1)	0.018(3)	0.228(1)	7.0(6)
C(15)	0.378(1)	−0.022(2)	0.2872(9)	6.1(6)
C(16)	0.351(1)	0.070(2)	0.3235(8)	4.5(5)
C(17)	0.155(1)	0.433(2)	0.4382(8)	4.6(5)
C(18)	0.085(1)	0.522(2)	0.4446(9)	5.7(6)
C(19)	0.079(1)	0.625(2)	0.4008(9)	5.8(6)
C(20)	0.104(1)	0.553(2)	0.3529(8)	4.2(5)
C(21)	0.120(1)	0.457(2)	0.2313(8)	4.5(5)
C(22)	0.119(1)	0.413(2)	0.173(1)	6.2(6)
C(23)	0.260(1)	0.452(2)	0.2659(8)	4.1(5)
C(24)	0.270(1)	0.599(2)	0.2835(9)	5.3(5)
C(25)	0.731(1)	0.224(2)	0.9010(7)	3.5(4)
C(26)	0.771(1)	0.280(2)	0.8648(7)	3.6(4)
C(27)	0.834(1)	0.216(2)	0.8559(8)	4.6(5)
C(28)	0.859(1)	0.088(2)	0.8804(8)	4.4(5)
C(29)	0.820(1)	0.028(2)	0.9122(8)	4.3(5)
C(30)	0.755(1)	0.094(2)	0.9243(8)	3.9(4)
C(31)	0.654(1)	0.465(2)	0.9008(7)	3.1(4)
C(32)	0.590(1)	0.535(2)	0.8795(8)	4.5(5)
C(33)	0.587(1)	0.683(3)	0.8746(9)	6.4(6)
C(34)	0.653(1)	0.747(2)	0.890(1)	6.2(6)
C(35)	0.722(1)	0.683(3)	0.911(1)	6.3(6)
C(36)	0.718(1)	0.540(2)	0.9178(8)	4.5(5)
C(37)	0.583(1)	0.224(2)	0.8716(7)	3.2(4)
C(38)	0.547(1)	0.107(2)	0.8881(8)	4.5(5)
C(39)	0.486(1)	0.037(2)	0.8455(9)	6.0(6)
C(40)	0.469(1)	0.079(2)	0.7969(9)	5.7(6)
C(41)	0.505(1)	0.187(2)	0.7812(9)	5.7(6)
C(42)	0.563(1)	0.263(2)	0.8177(8)	4.4(5)
C(43)	0.647(1)	0.286(2)	0.9746(7)	3.3(4)
C(44)	0.709(1)	0.255(2)	1.0165(7)	3.5(4)
C(45)	0.702(1)	0.248(2)	1.0696(8)	4.6(5)
C(46)	0.632(1)	0.272(2)	1.0818(8)	4.8(5)
C(47)	0.571(1)	0.304(2)	1.0410(9)	5.6(5)
C(48)	0.581(1)	0.311(2)	0.9874(8)	4.4(5)
B	0.654(1)	0.298(2)	0.9123(8)	3.0(4)

[a] $B_{eq} = 4/3\Sigma_i\Sigma_j\beta_{ij}\mathbf{a}_i\mathbf{a}_j$.

Table 5
Fractional atomic coordinates, thermal parameters and their estimated standard deviations for [U(COT)(S$_2$CNEt$_2$)(THF)$_2$][BPh$_4$]

	x	y	z	B_{eq}
U	0.1264(1)	0.23663(4)	0.03225(4)	3.54(2) [a]
S(1)	0.1375(7)	0.1925(3)	−0.0876(3)	4.8(2) [a]
S(2)	0.3216(9)	0.1382(3)	0.0108(3)	5.9(2) [a]
O(1)	0.348(2)	0.2556(7)	0.1011(6)	4.6(3)
O(2)	0.287(2)	0.3102(7)	−0.0179(7)	4.5(4)
N	0.336(2)	0.1011(9)	−0.1044(9)	5.6(5)
C(1)	−0.159(2)	0.244(1)	−0.006(1)	5.3(6)
C(2)	−0.144(3)	0.185(1)	0.022(1)	6.6(7)
C(3)	−0.078(3)	0.167(1)	0.081(1)	5.4(6)
C(4)	−0.015(3)	0.198(1)	0.129(1)	5.2(6)
C(5)	0.010(3)	0.256(1)	0.141(1)	5.8(6)
C(6)	−0.004(3)	0.311(1)	0.110(1)	8.4(9)
C(7)	−0.059(3)	0.330(1)	0.053(1)	7.4(8)
C(8)	−0.121(3)	0.301(1)	0.006(1)	6.3(7)
C(9)	0.261(3)	0.142(1)	−0.062(1)	4.3(5)
C(10)	0.293(3)	0.104(1)	−0.170(1)	5.6(6)
C(11)	0.380(3)	0.149(1)	−0.206(1)	6.1(7)
C(12)	0.449(3)	0.053(1)	−0.087(1)	5.9(7)
C(13)	0.369(3)	−0.007(1)	−0.070(1)	8.4(9)
C(14)	0.379(3)	0.313(1)	0.129(1)	7.3(8)
C(15)	0.534(3)	0.307(1)	0.154(1)	8.6(9)
C(16)	0.567(3)	0.242(1)	0.162(1)	7.8(7)
C(17)	0.433(3)	0.211(1)	0.137(1)	6.5(7)
C(18)	0.219(3)	0.355(1)	−0.061(1)	5.5(6)
C(19)	0.340(3)	0.372(1)	−0.101(1)	6.1(7)
C(20)	0.489(3)	0.355(1)	−0.068(1)	5.6(6)
C(21)	0.446(3)	0.300(1)	−0.033(1)	5.8(6)
C(22)	0.313(2)	0.1193(9)	0.2887(8)	2.4(4)
C(23)	0.409(2)	0.1642(9)	0.3079(9)	3.2(5)
C(24)	0.363(2)	0.227(1)	0.3154(9)	4.5(5)
C(25)	0.216(3)	0.239(1)	0.306(1)	5.9(6)
C(26)	0.113(3)	0.197(1)	0.288(1)	4.3(5)
C(27)	0.160(2)	0.1361(9)	0.2808(9)	3.2(5)
C(28)	0.272(2)	0.0112(9)	0.2291(8)	2.6(4)
C(29)	0.236(2)	0.042(1)	0.177(1)	4.2(5)
C(30)	0.171(3)	0.012(1)	0.126(1)	5.0(6)
C(31)	0.141(3)	−0.050(1)	0.130(1)	5.3(6)
C(32)	0.179(3)	−0.081(1)	0.181(1)	4.5(6)
C(33)	0.246(2)	−0.054(1)	0.229(1)	3.7(5)
C(34)	0.534(2)	0.0349(9)	0.2786(9)	2.7(4)
C(35)	0.618(2)	−0.0085(9)	0.3112(9)	3.3(5)
C(36)	0.772(2)	−0.018(1)	0.300(1)	4.0(5)
C(37)	0.848(3)	0.016(1)	0.257(1)	4.6(6)
C(38)	0.771(3)	0.059(1)	0.226(1)	4.4(5)
C(39)	0.621(3)	0.068(1)	0.234(1)	5.1(6)
C(40)	0.299(2)	0.0201(9)	0.3550(9)	2.9(5)
C(41)	0.163(2)	−0.010(1)	0.364(1)	4.1(5)
C(42)	0.116(3)	−0.025(1)	0.424(1)	5.7(6)
C(43)	0.191(3)	−0.009(1)	0.472(1)	6.0(7)
C(44)	0.328(2)	0.022(1)	0.466(1)	4.6(6)
C(45)	0.379(3)	0.034(1)	0.407(1)	3.9(5)
B	0.355(3)	0.046(1)	0.287(1)	2.8(5)

[a] $B_{eq} = 4/3\Sigma_i\Sigma_j\beta_{ij}\mathbf{a}_i\mathbf{a}_j$.

4.11. X-ray crystal structures of 9 and 15

Selected single crystals were introduced into thin-walled Lindemann glass tubes in the glove box. Data were collected on an Enraf–Nonius CAD-4 diffractome-

ter equipped with a graphite monochromator (λ(Mo Kα) = 0.70073 Å). The cell parameters were obtained by a least squares refinement of the setting angles of 25 reflections with θ between 8 and 12°. Three standard reflections were measured after every hour; a decay was observed (63% in 11 h for **9** and 16% in 60 h for **15**) and linearly corrected. The data were corrected for Lorentz polarization effects and absorption [26]. The structure was solved by the heavy-atom method and refined by full matrix least squares on F with anisotropic thermal parameters (U and S atoms for **9** and U atom for **15**); H atoms were not introduced. All calculations were performed on a Vax 4000-200 computer with the Enraf–Nonius MolEN system [27]. Analytical scattering factors for neutral atoms were corrected for both $\Delta f'$ and $\Delta f''$ components of anomalous dispersion [28]. Crystallographic data are given in Table 3 and final positional parameters in Tables 4 and 5.

References

[1] J.C. Berthet, C. Boisson, M. Lance, J. Vigner, M. Nierlich and M. Ephritikhine, *J. Chem. Soc. Dalton Trans.*, (1995) 3019.

[2] J.C. Berthet, C. Boisson, M. Lance, J. Vigner, M. Nierlich and M. Ephritikhine, *J. Chem. Soc. Dalton Trans.*, (1995) 3027.

[3] J. Feldman and J.C. Calabrese, *J. Chem. Soc. Chem. Commun.*, (1991) 134; G.C. Martin, G.J. Palenik and J.M. Boncella, *Inorg. Chem.*, 29 (1990) 2027; A.L. Casalnuovo, J.C. Calabrese and D. Milstein, *J. Am. Chem. Soc.*, *110* (1988) 110.

[4] D. Röttger, G. Erker, M. Grehl and R. Fröhlich, *Organometallics*, *13* (1994) 3897.

[5] C. Boisson, J.C. Berthet, M. Lance, J. Vigner, M. Nierlich and M. Ephritikhine, *J. Chem. Soc. Dalton Trans.*, (1996) 947.

[6] T. Arliguie, D. Baudry, M. Ephritikhine, M. Nierlich, M. Lance and J. Vigner, *J. Chem. Soc. Dalton Trans.*, (1992) 1019.

[7] J.C. Berthet, J.F. Le Maréchal and M. Ephritikhine, *J. Organomet. Chem.*, *480* (1994) 155.

[8] M.F. Lappert, P.P. Power, A.R. Sanger and R.C. Srivastava, *Metal and Metalloid Amides: Syntheses, Structures and Physical and Chemical Properties*, Ellis Horwood, Chichester, and Wiley, New York, 1980.

[9] G. Chandra, A.D. Jenkins, M.F. Lappert and R.C. Srivastava, *J. Chem. Soc. A*, (1970) 2550; D.C. Bradley and M.C. Ganorkar, *Chem. Ind.*, (1968) 1521.

[10] K. Jones and M.F. Lappert, *J. Organomet. Chem.*, *3* (1965) 295; M. Rivière-Baudet and P. Rivière, *J. Organomet. Chem.*, *116* (1976) C49.

[11] N.L. Allinger, M.P. Cava, D.C. De Jongh, C.R. Johnson, N.A. Lebel and C.L. Steven, *Chimie Organique*, Vol. 1, McGraw Hill, 1976.

[12] C. Boisson, J.C. Berthet and M. Ephritikhine, unpublished results.

[13] P.C. Leverd, T. Arliguie, M. Lance, M. Nierlich, J. Vigner and M. Ephritikhine, *J. Chem. Soc. Dalton Trans.*, (1994) 501.

[14] J.L. Stewart and R.A. Andersen, *New J. Chem.*, *19* (1995) 587.

[15] P.J. Fagan, J.M. Manriquez, T.J. Marks, C.S. Day, S.H. Vollmer and V.W. Day, *Organometallics*, *1* (1982) 170.

[16] W.G. Van Der Sluys, C.J. Burns and A.P. Sattelberger, *Organometallics*, *8* (1989) 855.

[17] C.K. Johnson, ORTEP II, *Rep. ORNL-5138*, 1976 (Oak Ridge National Laboratory, TN).

[18] K. Bowman and Z. Dori, *J. Chem. Soc. Chem. Commun.*, (1968) 636.

[19] M. Pennington, N.W. Alcock and D. Brown, *Inorg. Chim. Acta*, *139* (1987) 49.

[20] D. Brown, D.G. Holah and C.E.F. Rickard, *J. Chem. Soc. A*, (1970) 423.

[21] C.S. Harreld and E.O. Schlemper, *Acta Crystallogr. Sect. B:*, *27* (1971) 1964; S. Merlino, *Acta Crystallogr. Sect. B:*, *24* (1968) 1441.

[22] A.R. Shake, L.R. Avens, C.J. Burns, D.L. Clark, A.P. Sattelberger and W.H. Smith, *Organometallics*, *12* (1993) 1497.

[23] D. Baudry, E. Bulot, M. Ephritikhine, M. Nierlich, M. Lance and J. Vigner, *J. Organomet. Chem.*, *388* (1990) 279; T.R. Boussie, R.M. Moore, A. Streitwieser, A. Zalkin, J. Brennan and K.A. Smith, *Organometallics*, *9* (1990) 2010; A. Streitwieser and T.R. Boussie, *Eur. J. Solid State Inorg. Chem.*, *28* (1991) 399.

[24] P.J. Davidson, D.H. Harris and M.F. Lappert, *J. Chem. Soc. Dalton Trans.*, (1976) 2268.

[25] F.T. Edelmann, F. Pauer, M. Wedler and D. Stalke, *Inorg. Chem.*, *31* (1992) 4143.

[26] A.C.T. North, D.C. Phillips and F.S. Mathews, *Acta Crystallogr. Sect. A:*, *24* (1968) 351.

[27] *MolEN, An Interactive Structure Solution Procedure*, Enraf-Nonius, Delft, 1990.

[28] *International Tables for X-ray Crystallography*, Vol. IV, Kynoch, Birmingham, 1974 (present distributor: Academic, Dordrecht).